P2.17 INVESTIGATIONS OF LIQUID WATER PATH SPATIAL VARIABILITY USING MODIS

Robert Wood* and Dennis L. Hartmann
University of Washington, Seattle, Washington

1. Introduction

Boundary layer cloud structure is never homogenenous. Heterogeneities occur on all scales (e.g. Lovejoy 1982, Cahalan and Snider 1989, Kostinski and Shaw 2001) Two important points related to cloud heterogeneity are:

(i) a complete understanding of the convective processes driving the organisation and structure of marine boundary layer clouds has not yet been attained (see Atkinson and Zhang 1996). One approach to elucidating possible mechanisms for mesoscale cellular convection (MCC) is to characterise the types of cloud structures over large areas and couple this with synoptic data to examine statistical relationships between large-scale forcings and cloud structural properties;

(ii) models of boundary layer clouds do not explicitly resolve processes that are occurring on scales smaller than the grid-box size. Two processes of particular importance to climate are radiative transfer (Cahalan et al. 1994) and precipitation generation (Albrecht 1989). Both processes have non-linear relationships between local cloud properties (optical thickness, liquid water path) and the process variable of interest (albedo, precipitation rate). For any process that depends nonlinearly upon a local cloud property, using the mean value of the cloud property will result in an erroneous estimation of the mean value of the process (e.g. Pincus and Klein 2000). The mean short wave reflectance of a cloudy domain is always less for a heterogeneous cloud than for a homogeneous cloud. For precipitation rates this is reversed.

In this study we:

(i) examine MODIS data from both the Californian and Peruvian regions to assess characteristics of the spatial variability in marine boundary layer clouds;

(ii) estimate the dominant spatial scales and MCC characteristics of boundary layer clouds;

(iii) estimate the potential magnitudes of precipitation biases in climate models if cloud spatial variability is not accounted for.

2. Data analysis

Data from the Moderate Resolution Imagining Spectroradiometer (MODIS) on the recently launched Terra satellite are used to assess liquid water path characteristics in regions dominated by warm low-level clouds. From measurements of optical thickness and effective radius (King et al. 1997) it is possible to estimate (e.g. Brenguier et al. 2000) liquid water path and droplet concentration: parameters of more relevance to cloud microphysical processes. Spatial resolution is 1km. All MODIS images used are collected at approximately 10-11 AM local time.

3. Characteristics of spatial variability

To investigate the climatology of mesoscale cellular convection we need a measure of the convective cell characteristic lengthscale and to know if the convection is open or closed cellular in form. To investigate the likely magnitude of process rate biases requires knowledge of the moments of the pdf of the relevant cloud properties.

Here we use 2-D Fourier analysis on 256x256 km MODIS scenes to determine the spatial scaling in the LWP fields. Fig. 1 shows the method used to determine the dominant spatial scale of convective cells. After detrending the 2D LWP field by removing the best fit planar surface, the 2D power spectrum P_{LWP} is generated as a function of the combined wavenumber k, where $k^2 = k_x^2 + k_y^2$. Horizontal asymmetry information is therefore discarded. In Fig. 1 the power spectra are shown for three cases. Note how the characteristic convective cell size corresponds well to a peak in the power spectrum with an associated power-law energy cascade at smaller scales. However, automatically selecting the wavenumber of the peak from a noisy, multi-peaked signal proved to be more complicated than anticipated. We found that a reasonable method was to calculate a second characteristic lengthscale λ_0 (marked by solid triangles on the abscissae in Fig. 1) from P_{LWP} using

$$\lambda_0^{-1} = \int_0^\infty k P_{LWP} dk \qquad (1)$$

We found by inspection that λ_0 itself is not a particularly good measure of the scale of the convective cells because it is too heavily dependent upon the power spectrum at larger scales which are poorly sampled. However, when a power-law fit to the spectrum for $k > 1.5/\lambda_0$ is calculated, this generally fits the energy cascade region of the spectrum well (dotted straight line in Fig. 1). The peak scale is then determined by first binning P_{LWP} using logarithmically spaced bins (filled circles) and calculating the 95% confidence limits (dotted curves). We determine the convective cell scale λ as the inverse of the wavenumber at which the upper confidence limit falls below the power-law fit, i.e. the smallest scale at which the observed power spectrum deviates at the 95% level from the power-law (vertical dashed lines). Note that in (a) there is no scale for which

* *Corresponding author address*: Dr. Robert Wood, Atmospheric Sciences, University of Washington, Seattle, WA; *e-mail: robwood@atmos.washington.edu.*

this criterion is fulfilled. We find that in almost all these cases of failure (<5% of total scenes processed), the peak in the power spectrum is located at small scales (<5-10 km), which is close to the Nyquist scale (2km). For cases (b) and (c) the derived cell scales are 10.3 and 48.2 km, which are in good agreement with those chosen by visual inspection.

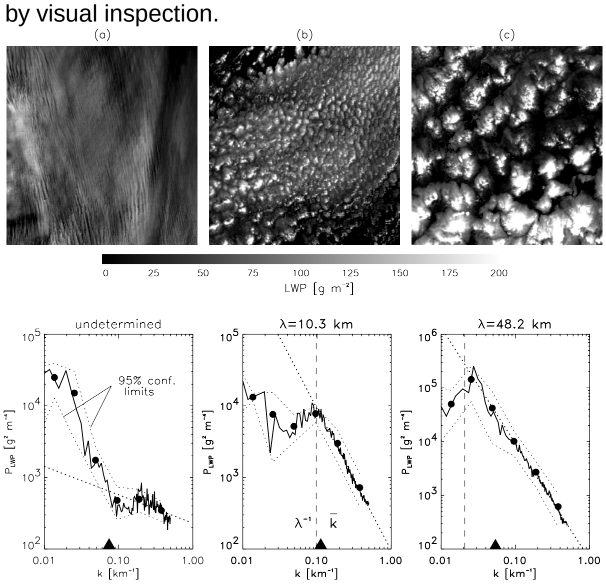

Figure 1: *Example showing LWP power spectra used to determine the dominant spatial scale of the MCC.*

The LWP pdf is derived for the cloudy pixels in each scene. The pdf and the power spectrum are used to classify scenes as containing open cellular, closed cellular or homogeneous cloud. Open cellular convection has more skewed pdfs and more power at small scales (P_{small}, the integrated power for $0.2 < k < 0.5$ km^{-1}). Closed and open MCC cannot be diagnosed based upon cloud fraction alone because closed cellular convection covering only a small portion of the scene would be misdiagnosed as open celled convection. Fig. 2 shows an example of the diagnosis of open and closed cells. We diagnose open cellular convection as having (a) skewness larger than 1.8; (b) $P_{small} > 250$ g^2 m^{-4}; (c) cloud fraction $0.1 < CF < 0.75$. Of the remaining scenes, those with $\lambda > 10$ km and $CF > 0.1$ are classified as closed cellular convection. Those with $\lambda \leq 10$ km and $CF > 0.1$ are classified as homogeneous cloud. Finally, those with $CF < 0.1$ are unclassified. These could either be scattered trade with cumulus or edges of extensive stratocumulus.

4. Frequencies and scales of cellular convection

Fig. 3 shows the freqeuncies of homogeneous, open and closed MCC for the Californian and Peruvian regions during SON. Close to the Calfornian coast homogeneous and closed cellular convection dominate. Close to the S. American coast there is less homogeneous cloud and more closed cells (over 90% in places) which most likely reflects the deeper boundary layers found close to the S. American coast. There is also an interesting band

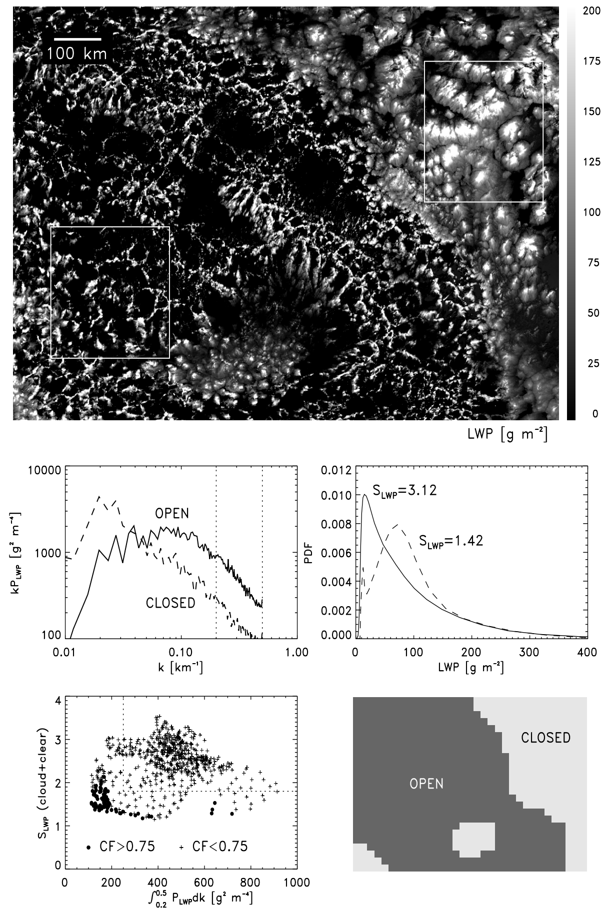

Figure 2: *Diagnosis of open/closed cellular convection. Two example scenes are chosen from larger image (top). Second row shows LWP power spectra and pdfs. Third row shows small scale power plotted against skewness (see text), and location of where open and closed cellular convection has been diagnosed in upper image.*

of closed MCC just south of the equator where equatorial upwelling is prevalent. Open MCC dominates further westwards in the subtropical regions.

Spatial scales of the closed MCC are shown in Fig. 4. The median λ for the closed MCC is 26.1 and 24.2 km for the Californian and Peruvian regions respectively. There is a tendency for the integral scale to underpredict the cell sizes for open MCC and so these are not presented.

Convective cell scales increase with distance away from the coast in the Californian region, while the largest cells are typically found close to the S. American coast. The reason for this is not yet clear although one might expect that the cell diameter would scale with the depth of the boundary layer. Accurate MODIS cloud top temperatures have only recently become available; we will examine cell scaling relationships as this data becomes available.

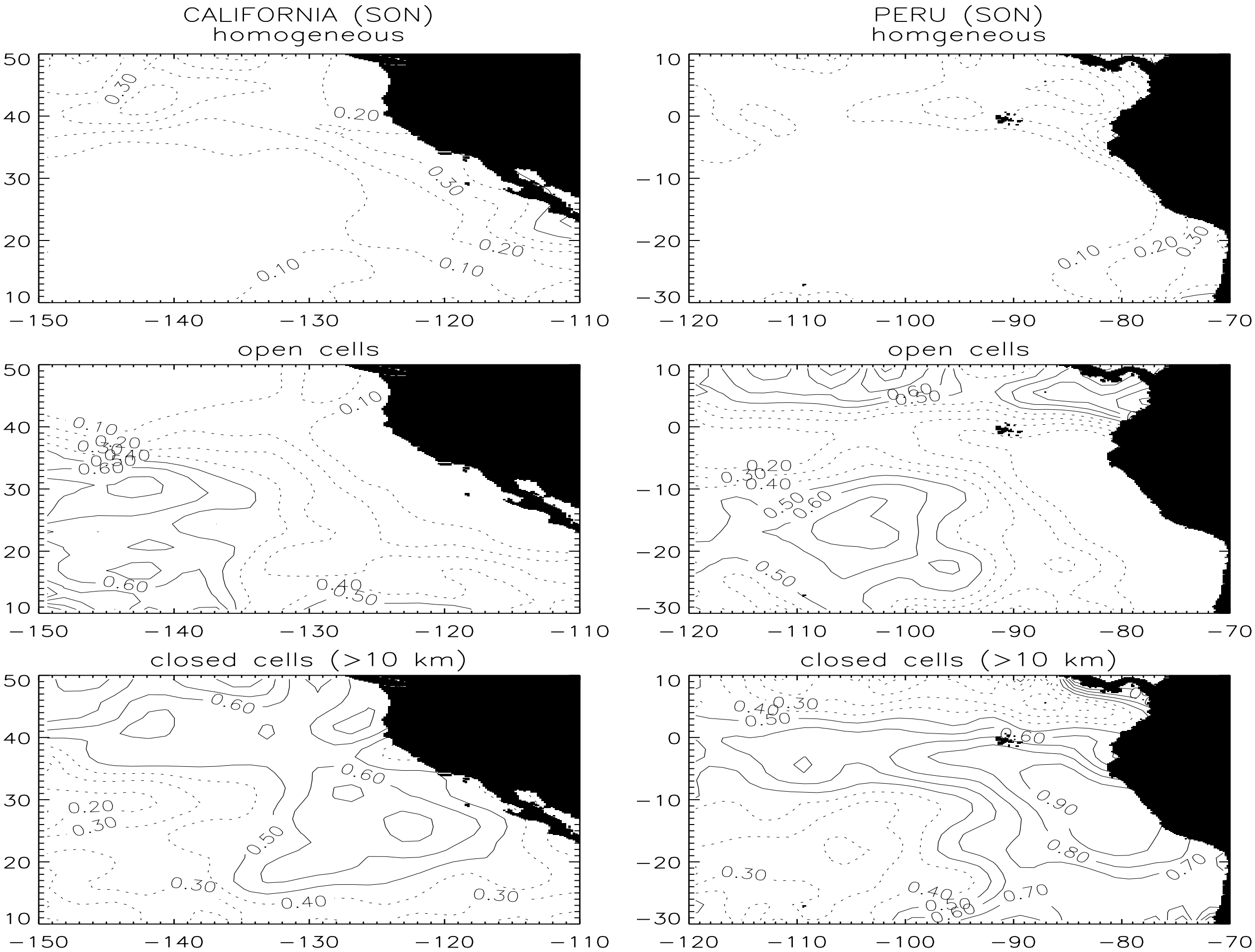

Figure 3: *Diagnosed homogeneous, open and closed cellular convection frequencies for Californian and Peruvian regions during SON.*

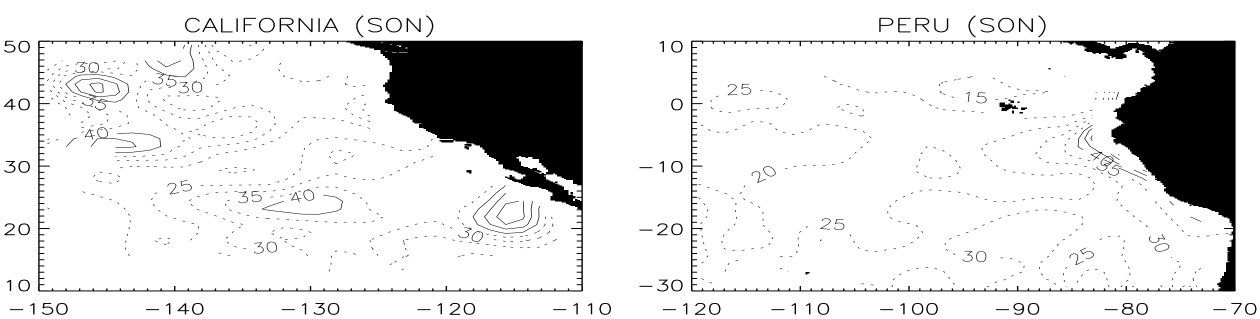

Figure 4: *Median integral scale of closed cells.*

5. LWP and precipitation variability

The role of precipitation in controlling the distribution of liquid water within boundary layer clouds remains uncertain. The dependence of drizzle rate upon liquid water content and droplet concentration is not quantitatively known with any accuracy. Here, we present a simple model which can be used to examine precipitation rate variability in warm boundary layer clouds. The model is a simple one dimensional equilibrium model which models drizzle formation through the processes of autoconversion, accretion and sedimentation. The model has been used to assess the merits of various autoconversion and accretion schemes. Fairly good agreement between modelled and observed precipitation rates is obtained when the Khairoutdinov and Kogan (2000) parameterisations for autoconversion, accretion and sedimentation are used.

The assumption is made that the cloud liquid water content and droplet concentration profiles do not change with time, i.e. the precipitation flux is balanced by the moisture flux into the cloud through the base and top. This may be a reasonable approximation for stratocumulus with moderate amounts of drizzle where observations suggest that the profiles of liquid water content remain fairly adiabatic.

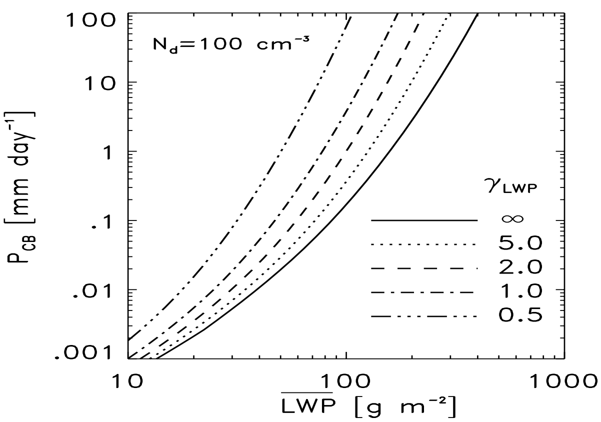

Figure 5: *Mean cloud-base precipitation rate as a function of $\overline{LWP}$ and γ_{LWP}. Droplet concentration is 100 cm^{-3}.*

The LWP pdf is well represented using a Gamma distribution (two free parameters). Using this the precipitation rate at cloud base is calculated for inhomogeneous clouds with different $\overline{LWP}$ and γ_{LWP}, where $\gamma_{LWP} = (\overline{LWP}/\sigma_{LWP})^2$. The domain size is 256x256 km. For a given $\overline{LWP}$ clouds with higher levels of heterogeneity (lower γ_{LWP}) have higher mean cloud base precipitation rates (Fig. 5). This is because the autoconversion rate has a strongly non-linear dependence upon cloud liquid water content. Thus a bias is introduced if the cloud is assumed to be homogeneous (e.g. Pincus and Klein 2000). This bias can be significant. For the dataset median $\overline{LWP} = 80$ g m^{-2} and $\gamma_{LWP} = 1.0$, the heterogeneous mean cloud base precipitation rate P_{CB} is a factor of 11.6 higher than the rate P_{PPH} calculated for a plane parallel homogeneous cloud. Biases become greater at higher values of $\overline{LWP}$ because at higher cloud liquid water contents the accretion term amplifies biases in autoconversion rates.

The geographical distribution of the precipitation bias $(P_{CB} - P_{PPH})/P_{PPH}$ is shown in Fig. 6. The estimated biases are smallest (< 5) where there is a prevalence of relatively homogeneous stratus clouds close to the N. and S. American coastlines. Even here however, the biases are not negligible. Further from the coast in the transition/cumulus regions, the biases can become very large.

6. Conclusions

Early data have been presented from the MODIS instument, which are being used to investigate cloud spatial inhomogeneity characterised using power spectra and pdfs. Diagnosis of the type of convection and the scales of the cells will be used to determine the synoptic conditions for the formation of MCC. The width of the LWP pdf is important in determining the mean cloud base precipitation rate for a given area of heterogeneous cloud. All GCMs use a plane parallel (PPH) homogeneous model for calculating precipitation. A simple model to account for cloud spatial variability suggests that the PPH assumption can result in considerable underprediction of drizzle rates.

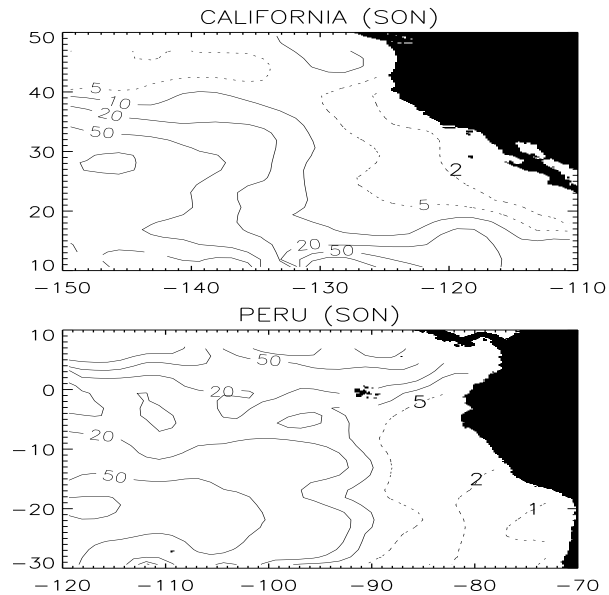

Figure 6: *Median precipitation rate biases*

References

Albrecht, B. A., (1989): Aerosols, cloud microphysics and fractional cloudiness. *Science*, **245**, 1227-1230.

Atkinson, B. W. and J. Wu Zhang, 1996: Mesoscale shallow convection in the atmosphere. *Rev. Geophys.*, **34**, 403-431.

Brenguier, J.-L., H. Pawlowska, L. Schuller, R. Preusker, J. Fischer, Y. Fouquart, 2000: Radiative properties of boundary layer clouds: droplet effectvie radius versus number concentrations, *J. Atmos. Sci.*, **57**, 803-821.

Cahalan, R. F. and J. B. Snider, 1989: Marine statocumulus structure, *Remote Sens. Environ.*, **28**, 95-107.

Cahalan, R. F., W. Ridgway, W. J. Wiscombe, T. L. Bell, J. B. Snider, 1994: The albedo of fractal stratocumulus clouds, *J. Atmos. Sci.*, **51**, 2434-2460.

Khairoutdinov, M. and Y. Kogan, 2000: A new cloud physics parameterization in a large-eddy simulation model of marine stratocumulus. *Mon. Wea. Rev.*, **128**, 229-243.

King, M. D., S-C. Tsay, S. E. Platnick, M. Wang, K-N. Liou, 1997: Cloud retriveal algorithms for MODIS. Optical thickness, effective particle radius, and thermodynamic phase. *MODIS Algorithm Theoretical Basis document No. ATBD-MOD-05*, NASA.

Kostinski, A. B. and R. A. Shaw, 2001: Scale-dependent droplet clustering in turbulent clouds. *J. Fluid. Mech.*, **434**, 389-398.

Lovejoy, S. D., 1982: The area-perimeter relationship for rain and cloud areas, *Science*, **216**, 185-187.

Pincus, R. and S. A. Klein, 2000: Unresolved spatial variability and microphysical process rates in large-scale models. *J. Geophys. Res.*, **105**, 27059-27065.